Perspicacious indicators of atmospheric blocking

C. Schwierz, M. Croci-Maspoli, and H. C. Davies

Institute for Atmospheric and Climate Science, Eidgenossische Technische Hochschule, Zürich, Switzerland

Received 20 December 2003; revised 9 February 2004; accepted 25 February 2004; published 27 March 2004.

[1] A novel dynamically-based approach is introduced to identify, describe and diagnose atmospheric blocking events. The approach is based upon the potential vorticity perspective and takes into account the three-dimensional structure of the phenomenon. It is argued that the essence of a blocking anomaly is located in the upper troposphere, just below the tropopause. The associated novel blocking indicators are derived from two-dimensional fields at 6-hourly temporal resolution, and provide information on the spatial scale, shape, amplitude and movement of blocks. A northern hemisphere winter (DJF) climatology for the ERA15 period (1979–1993) is presented and comments are made on the relationship between the indicators and previous blocking indices. *INDEX TERMS:* 3309 Meteorology and Atmospheric Dynamics: Climatology (1620); 3300 Meteorology and Atmospheric Dynamics; 3319 Meteorology and Atmospheric Dynamics: General circulation; 3364 Meteorology and Atmospheric Dynamics: Synoptic-scale meteorology. **Citation:** Schwierz, C., M. Croci-Maspoli, and H. C. Davies (2004), Perspicacious indicators of atmospheric blocking, *Geophys. Res. Lett.*, *31*, L06125, doi:10.1029/2003GL019341.

1. Introduction

[2] Atmospheric blocking events are sustained, vertically coherent, and quasi-stationary synoptic-scale high-pressure systems in the extratropics whose amplitude is such that they disrupt the prevailing westerly circumpolar flow. They exert a strong impact upon the upstream, in-situ, and downstream weather patterns and thereby constitute a significant climatological feature. It follows that understanding this phenomenon is a key dynamical challenge, and its accurate prediction a highly desirable goal for medium- and seasonal-range forecasting.

[3] An abiding research theme is the study of their climatology (for a historical overview see *Sausen et al.* [1995], hereinafter referred to as SKS95), and yet there is no generally accepted objective definition (sic. index) of a block [*Liu*, 1994]. Some early indices used the 500 hPa geopotential height surface, and were based upon (a) the identification of distinctive synoptic-scale closed or Ω-shaped high pressure systems that matched prescribed blocking patterns [*Sumner*, 1954], (b) the determination of major positive height anomalies [*Dole and Gordon*, 1983] or (c) a localized positive latitudinal gradient of the geopotential field connoting an in-situ easterly geostrophic flow [*Lejenäs and Økland*, 1983; *Tibaldi and Molteni*, 1990] (hereinafter referred to as TM90). In contrast a recently proposed index used the potential temperature (θ) field on the dynamic tropopause (TP), sic. 2 pvu surface, to pinpoint the location of a reversal of the customary negative latitudinal θ-gradient and thereby to indicate a localized quasi-horizontal wave-overturning on the TP [*Pelly and Hoskins*, 2003] (hereinafter referred to as PH03).

[4] In principle the formulation of a dynamically-based index should be consistent with the phenomenon's salient features including its spatial-scale and structure, amplitude, life cycle and duration, movement and geographical location. Such an index would yield a comprehensive blocking climatology incorporating the forementioned features, and could in turn shed light on the instigation, maintenance, break-down, and categorization of blocks. In practice the selection of an index for a particular study has been constrained by the available data sets, the specific objective(s) of the study, and often the desirability of deploying efficient algorithms for automatic identification of blocks.

[5] Here we introduce two related novel indicators of blocking that are formulated in a potential vorticity (PV) framework. In this framework the phenomenon is to be viewed in terms of the evolution and pattern of its PV distribution. Previous studies that have examined blocks in this framework include consideration of the associated adiabatic [*Shutts*, 1986; *Swanson*, 2001], and diabatic [*Schwierz*, 2001] PV transport.

[6] In the following sections we set out the rationale and the methodology for computing the new indicators (section 2), display and discuss the geographical distribution of winter season blocking events computed using the indicators (section 3), and comment on their distinctive properties (section 4).

2. Approach and Methodology

2.1. Rationale

[7] To illustrate the ingredients of the proposed index we compare conventional depictions of a block with analogue PV-based fields. Figure 1 displays conventional instantaneous pseudo-horizontal and vertical sections through one particular block located over the Western-Atlantic in January 1981. Note that the data for these depictions (and all other components of the present study) were derived from the ECMWF ERA-15 data set [*Gibson et al.*, 1996] for the time period 1979–1993, and an anomaly is defined relative to the corresponding 15-year monthly mean value.

[8] The pseudo-horizontal fields (Figure 1a) capture the standard forementioned blocking characteristics. In the vertical section (Figure 1b) the anomaly has an equivalent barotropic signature with a maximum at about 200 hPa. The barotropy lends support to the customary practice of adopting an index based upon the 500 hPa field, whilst the height

0094-8276/04/2003GL019341$05.00

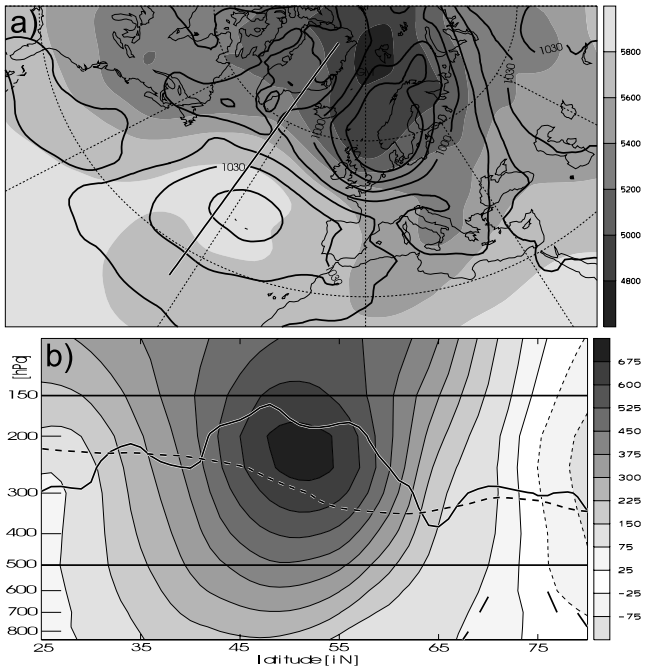

Figure 1. (a) 500 hPa geopotential height (Z, shaded, interval 200 m) and SLP isolines (black, interval 10 hPa) for 14 January 1981 18 UTC. (b) Cross section of Z anomaly at 33W from 25N–80N. Tropopause (PV = 2 pvu, bold solid) and pressure levels (150, 500 hPa) overlaid (black contours). Climatological tropopause (bold dashed).

of the maximum calls into question the optimality of that choice.

[9] An analogue of Figure 1a is the PV field on the 330 K isentropic surface (Figure 2a) and it shows a quasi-circular region of low PV co-located with the high pressure system and almost encircled by a ring of higher PV. This distribution equates in part to a poleward incursion of sub-tropical air resulting in a quasi-wave-breaking pattern, but there is only a limited correspondence to the oft-invoked dipolar representation of a block [e.g., *Haines and Marshall*, 1987]. The vertical section (Figure 2b) displays a PV anomaly field ($PV^{\star}$) defined by $PV^{\star} = PV - \overline{PV}$, where $\overline{PV}$ denotes the 15-year January monthly mean of the in-situ PV field. This anomaly field has a domain of strong negative values confined predominantly to the upper troposphere beneath an elevated TP.

[10] The $PV^{\star}$ variable introduced above and the dynamical feature captured in Figure 2b form the kernel for one of our proposed blocking indicators. The variable prescribes the instantaneous departure of the PV field away from its in-situ climatological value (i.e., $\overline{PV}$). It is linked, via the concept of PV inversion, to the departure of the thermal and flow fields away from their climatological distribution. Hence, consistent with the $PV^{\star}$ signature in Figure 2b, the accompanying isentropes are elevated above and depressed below the anomaly. Likewise the anomaly connotes anticyclonic circulation with the easterlies on its southern rim countering the in-situ climatological mean (sic. $\overline{PV}$-related) flow. More trenchantly, from a PV perspective, the negative $PV^{\star}$ anomaly's amplitude, horizontal scale and vertical confinement signifies that it is related directly to and can account for the block.

2.2. The Indicators

[11] Herein a block is identified as a persistent and significant quasi-isolated feature of low *PV* (as in Figure 2a) and/or a negative $PV^{\star}$ anomaly (as in Figure 2b). The specification and computation of the associated indices is undertaken in a three-step process. First the mean column-averaged value of both *PV* and $PV^{\star}$ from mid-tropospheric (500 hPa) to lower stratospheric (150 hPa) elevations [cf. *Shapiro and Donall-Grell*, 1994] are evaluated every six hours for the entire fifteen-year ERA period. In effect this procedure delivers horizontal fields whose pattern represents the instantaneous vertically-averaged *PV* and $PV^{\star}$ fields. (Note that the column average could be performed alternatively between two isentropic surfaces, e.g., 315 K and 330 K). At each time slot the local value of the variables are subjected to a two day running-mean time filter to smooth out the higher frequency components. The resulting fields are referred to hereafter as *APV* and $APV^{\star}$.

[12] *Second* the two types of smoothed six-hourly fields are scanned for closed contours that engulf respectively low (negative) values of *APV* ($APV^{\star}$) subject to some prescribed thresholds. This thresholding approach is akin to that used in earlier studies, but here we note that the dependency upon the specified threshold values provides additional climatological information (threshold values of <1.0 (−1.2) pvu correspond for example to the lower ~10% of the extratropical *APV* ($APV^{\star}$) distributions). In line with the main inference of the previous sub-section each retained

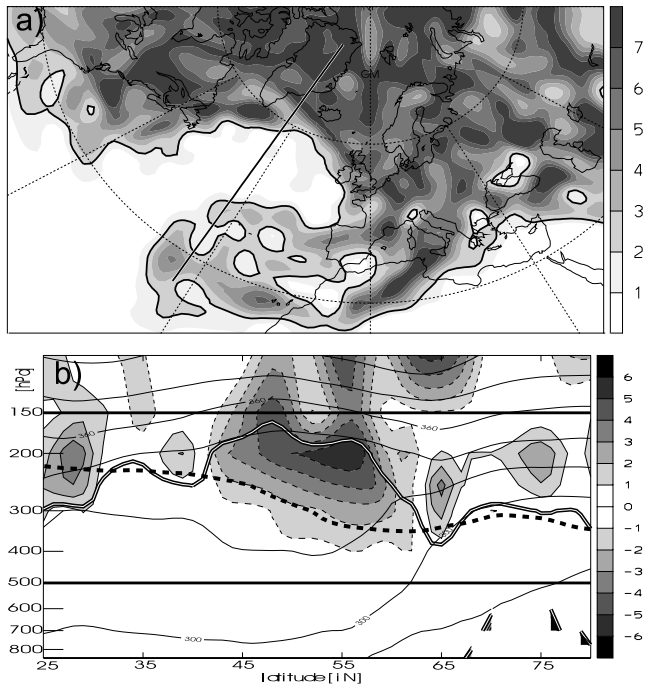

Figure 2. Analogous to Figure 1 for (a) Ertel PV on the 330 K isentrope (shaded, interval 1 pvu) and (b) cross section of PV anomaly at 33 W (shaded, interval 1 pvu, negative dashed). Lines denoting the instantaneous and climatological TP as in Figure 1. Thin contours in (b) indicate the θ distribution.

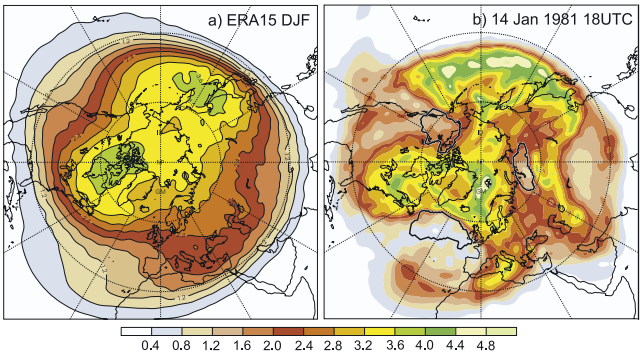

Figure 3. *APV* (PV average between 150 and 500 hPa) distributions (a) for the ERA15 DJF period (shaded, interval 0.4 pvu), and (b) on 14 January 1981 18 UTC (shaded) with closed *APV* anomaly ($APV^{\star}$) contours overlaid (black).

cut-off is viewed as a candidate for categorization as a block.

[13] *Third* a tracking algorithm is used to identify the temporal coherence of a cut-off by imposing a requirement of a specified percentage spatial overlap of the encircling contours between each six hour time-slot. In addition statistics are compiled of the geographical distribution, spatial scale, asymmetry and temporal coherence of each individual cut-off. It follows that a climatology can be derived for cut-offs satisfying specified amplitude (A), overlap (O), spatial scale (S) and duration (D) criteria for *APV* or $APV^{\star}$. In addition an examination can be undertaken of the climatology's sensitivity to the values of these various specified parameters (not shown here).

[14] Note that *APV* and $APV^{\star}$ cut-offs occurring in a region of uniform $\overline{PV}$ would be dynamically equivalent. In contrast in a region of strong $\overline{PV}$ gradient, an $APV^{\star}$ cut-off can occur although an *APV* closed contour might not be present. Such an event would connote an Ω-shaped pattern in the *APV* field.

[15] Further insight on the nature and efficacy of the indicators can be gleaned from inspection of the winter-season climatological $\overline{APV}$ field (Figure 3a), and the instantaneous depictions of the *APV* and $APV^{\star}$ fields (Figure 3b). The climatological field (Figure 3a) possesses a non-uniform latitudinal gradient with a band of enhanced gradient in the extratropics that itself has maxima over the eastern seaboard of Asia and North America. This band is aligned with the climatological TP-break, jet-stream and band of enhanced PV gradient on TP-intersecting isentropic surfaces [*Schwierz et al.*, 2004]. It is in effect the seat for baroclinic development. Likewise its variance (not shown) is located downstream of the forementioned maxima over the eastern continental seaboards, and is co-aligned with and mirrors the storm track pattern. It also follows that large-amplitude negative $APV^{\star}$ cut-offs resulting from isentropic transport of PV will have a predilection to evolve on the poleward fringe of the band of enhanced $\overline{APV}$ gradient and downstream of its two longitudinal maxima. In effect the band of enhanced $\overline{APV}$ gradient constitutes a longitudinally varying and dynamically determined base-latitude for examining the occurrence of blocks. Notwithstanding an $APV^{\star}$ cut-off can also occur at a latitude removed from the enhanced band provided isentropic stirring and/or diabatic processes suffice to produce a localized minimum at such a location.

[16] Figure 3b is the analogue of Figures 1a and 2a but now for the instantaneous *APV* and $APV^{\star}$ fields respectively. For the *APV* field the tilted Ω-shaped pattern in the Western Atlantic suggests that the block is a major but non-sequestered poleward excursion of sub-tropical air.

[17] In contrast there is a clearly identifiable cut-off in the $APV^{\star}$ field located slightly poleward of the block captured in the geopotential field (cf. Figure 1a). The analysis procedure set out above also indicates that this $APV^{\star}$ feature satisfies the forementioned temporal coherency, scale and duration criteria. Thus in the present formulation the feature in the Western Atlantic can be categorized as a block in the $APV^{\star}$ field.

3. Sample Blocking Climatologies

[18] A climatology of the geographical distribution of the *APV*- and $APV^{\star}$-blocks are shown in Figure 4 for the three month (DJF) winter-seasons of the ERA-15 period (1979–1993). For this illustrative example the two types of blocks are subject to threshold values (see subsection 2.2) corresponding to: A < 1.0 pvu (−1.2 pvu); O ≥ 50% (70%); S > 1.0 (1.8) · 10^6 km^2 and D ≥ 5 days for *APV* ($APV^{\star}$). Note that at every time slot of a block's existence the entire area of the blocking is taken into account so that a 1% frequency at a particular location corresponds essentially to one blocked day per season.

[19] It is evident that, for the specified threshold values, *APV*-blocks are confined exclusively to the Atlantic-European sector, and are comparatively rare events (frequency ≤2.5%). The inference is that these events of presumed major sequestration of sub-tropical air into the extratropics constitute a special category, and thus their existence invites further study.

[20] In contrast $APV^{\star}$-blocks are prevalent over major swathes of the extra-tropical Northern Hemisphere and in particular over the Atlantic and Pacific Oceans. There are major maxima over the central Atlantic and the northwest Pacific (frequencies ∼12%). In line with our earlier assertions the preferred blocking locations are aligned along, and slightly poleward and downstream of, the band of enhanced $\overline{APV}$ gradient (cf. Figure 3a). This association links the blocking distribution very closely to the storm track pattern,

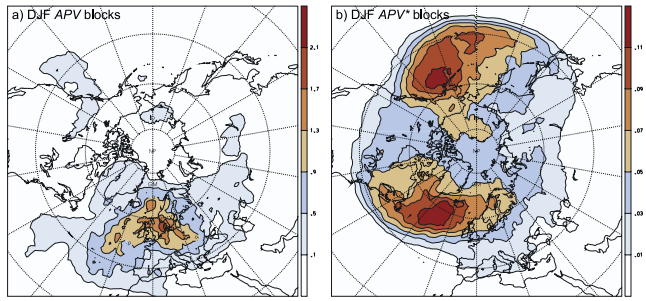

Figure 4. Winter season (DJF) frequency of (a) *APV*-blocks and (b) $APV^{\star}$-blocks, defined as the ratio of the number of blocked days to the total number of days per season. Note the different scales in a) and b).

although our blocking indicator does not incorporate direct information of the storm track pattern.

[21] There are several interesting aspects of the $APV^{\star}$-block climatology. These include the hint of a secondary maximum in mid-Pacific, the poleward extension of the blocking pattern beyond the Aleutian Islands, and the limb of enhanced activity over Labrador. Further analysis of both blocking types can also readily reveal the robustness of the climatological patterns to the precise values specified for the various threshold and space-time criteria.

[22] Figure 4 also serves as a basis for a comparison with climatologies derived with other indices. In particular the climatology of $APV^{\star}$-blocks (see Figure 4b) obtained with the forementioned stipulated criteria can be compared with: (a) the single-latitude results obtained using the Tibaldi-Molteni (TM) index, (b) the latitude-longitude distribution derived by SKS95, and (c) the wave-overturning statistics in the vicinity of the longitudinally-varying storm track of PH03. Co-comparison indicates a reasonable qualitative agreement in the geographical blocking distributions but with two notable discriminating features. First the present indicator's Atlantic maximum resembles only that recorded in the SKS-climatology as opposed to the maximum located east of the zero meridian in the other two climatologies. Recall however that the *APV*-block climatology (see Figure 4a) has its maximum at this longitude. Second the weak secondary maximum near the date-line is replicated with the TM-index whereas significant frequency in this longitudinal sector are only recorded with the PH-index if it is applied at 50N, rather than at the latitude of the storm track. The latter result, taken in conjunction with the present climatology's pinpointing of $APV^{\star}$-blocks in this sector, indicates a decoupling of the blocks from the prevailing storm track and that the dynamics of these blocks might be distinctive. Quantitatively the present indicator compares favourably with both the TM- and the SKS-indices, but registers reduced frequencies in comparison with the PH-index.

4. Further Remarks

[23] In generic terms the *APV* indicator identifies blocks with a distinctive synoptic structure [cf. *Sumner*, 1954; *Pelly and Hoskins*, 2003] and the $APV^{\star}$ indicator identifies significant departure away from the in-situ climatology [*Dole and Gordon*, 1983]. They do not account explicitly for an easterly geostrophic flow (cf. TM90). Notwithstanding a large-scale weak *APV* feature or a strong negative $APV^{\star}$ feature connote a significant weakening or even reversal of the ambient westerly flow on their equatorward fringe.

[24] These new PV-based indicators contrast with the extant indicators in several specific ways. They take into explicit account a seminal feature of the 3D atmospheric state via the column integration of PV. They incorporate intrinsically a longitude-dependent measure of the potential for blocking via the background $\overline{APV}$ climatology. They deliver a latitude-longitude distribution of blocking, and contemporaneously provide information on the amplitude, spatial scale, shape, and movement of blocks. More specifically, the *APV* cut-offs indicate the rare occurrence of entirely sequestered blocks such as those diagnosed herein to occur in the Atlantic sector. In contrast the anomaly field $APV^{\star}$ constitutes a more general measure that can represent persistent wave-undulations or Ω-type blocking events, and can be modified by PV advection.

[25] The attendant climatologies (Figure 4) bear comparison with, and shed light upon, those derived with other indices. Also the approach is such that it can be used to study the blocking climatology of numerical weather prediction and climate models, and to study trends in longer-term data sets such as the ERA 40. Intrinsic to the PV-based indicators is the identification of a block as a major upper-tropospheric negative PV anomaly, and this prompts alternative avenues to examine the dynamics of blocks. In particular it invites consideration of the origin, maintenance and the fate of such anomalies. For example an assessment can be made of the relative contributions of quasi-isentropic wave-breaking versus cloud-diabatic effects in the formation and maintenance of the PV anomaly [*Schwierz*, 2001].

[26] **Acknowledgments.** We thank ECMWF and MeteoSwiss for providing access to the ERA-15 data set, and acknowledge that the study was funded in part through the Swiss NCCR Climate Programme.

References

Dole, R. M., and N. D. Gordon (1983), Persistent anomalies of the extratropical Northern Hemisphere wintertime circulation: Geographical distribution and regional persistence characteristics, *Mon. Weather Rev.*, *111*, 1567–1586.

Gibson, J. K., et al. (1996), The ECMWF Re-Analysis (ERA) project, *Eur. Cent. Medium-Range Weather Forecasting Newslett.*, *73*, 7–17.

Haines, K., and J. Marshall (1987), Eddy-forced coherent structures as a prototype of atmospheric blocking, *Q. J. R. Meteorol. Soc.*, *113*, 681–704.

Lejenäs, H., and H. Økland (1983), Characteristics of Northern Hemisphere blocking as determined from a long time series of observational data, *Tellus, Ser. A*, *35*, 350–362.

Liu, Q. (1994), On the definition and persistence of blocking, *Tellus, Ser. A*, *46*, 286–298.

Pelly, J., and B. Hoskins (2003), A new perspective on blocking, *J. Atmos. Sci.*, *60*, 743–755.

Sausen, R., W. König, and F. Sielmann (1995), Analysis of blocking events from observations and ECHAM model simulations, *Tellus, Ser. A*, *47*, 421–438.

Schwierz, C. (2001), Interactions of Greenland-scale orography and extratropical synoptic-scale flow, Ph.D. dissertation, 155 pp., Eidg. Tech. Hochsch., Zurich, Switzerland.

Schwierz, C., S. Dirren, and H. C. Davies (2004), Forced waves on a zonally-aligned jet stream, *J. Atmos. Sci.*, *61*, 73–87.

Shapiro, M. A., and E. Donall-Grell (1994), In search of synoptic/dynamic conceptualizations of the life cycles of fronts, jet streams, and the tropopause, in *Proceedings of the International Symposium on the Life Cycles of Extratropical Cyclones*, edited by S. Grønås and M. A. Shapiro, pp. 163–181, Univ. of Bergen, Bergen, Norway.

Shutts, G. J. (1986), A case-study of eddy forcing during an Atlantic blocking episode, *Adv. Geophys.*, *29*, 135–162.

Sumner, E. J. (1954), A study of blocking in the Atlantic-European sector of the Northern Hemisphere, *Q. J. R. Meteorol. Soc.*, *80*, 345, 402–416.

Swanson, K. L. (2001), Blocking as a local instability to zonally varying flows, *Q. J. R. Meteorol. Soc.*, *127*, 1341–1355.

Tibaldi, S., and F. Molteni (1990), On the operational predictability of blocking, *Tellus, Ser. A*, *42*, 343–365.

M. Croci-Maspoli, H. C. Davies, and C. Schwierz, Institute for Atmospheric and Climate Science, ETH, CH-8093 Zürich, Switzerland. (schwierz@env.ethz.ch)